LRH-1–dependent glucose sensing determines intermediary metabolism in liver

Maaike H. Oosterveer,[1] Chikage Mataki,[1] Hiroyasu Yamamoto,[1] Taoufiq Harach,[1] Norman Moullan,[1] Theo H. van Dijk,[2] Eduard Ayuso,[3] Fatima Bosch,[3] Catherine Postic,[4] Albert K. Groen,[2] Johan Auwerx,[1] and Kristina Schoonjans[1]

[1]Institute of Bioengineering, School of Life Sciences, Ecole Polytechnique Fédérale de Lausanne, Lausanne, Switzerland. [2]Department of Pediatrics and Laboratory Medicine, Center for Liver, Digestive, and Metabolic Diseases, University Medical Center Groningen, University of Groningen, Groningen, The Netherlands. [3]Center of Animal Biotechnology and Gene Therapy and Department of Biochemistry and Molecular Biology, School of Veterinary Medicine, Universitat Autònoma de Barcelona Bellaterra, and CIBER de Diabetes y Enfermedades Metabólicas Asociadas, Barcelona, Spain. [4]Institut Cochin Inserm, Université Paris Descartes, Département d'Endocrinologie, Métabolisme et Cancer, Paris, France.

Liver receptor homolog 1 (LRH-1), an established regulator of cholesterol and bile acid homeostasis, has recently emerged as a potential drug target for liver disease. Although LRH-1 activation may protect the liver against diet-induced steatosis and insulin resistance, little is known about how LRH-1 controls hepatic glucose and fatty acid metabolism under physiological conditions. We therefore assessed the role of LRH-1 in hepatic intermediary metabolism. In mice with conditional deletion of *Lrh1* in liver, analysis of hepatic glucose fluxes revealed reduced glucokinase (GCK) and glycogen synthase fluxes as compared with those of wild-type littermates. These changes were attributed to direct transcriptional regulation of *Gck* by LRH-1. Impaired glucokinase-mediated glucose phosphorylation in LRH-1–deficient livers was also associated with reduced glycogen synthesis, glycolysis, and de novo lipogenesis in response to acute and prolonged glucose exposure. Accordingly, hepatic carbohydrate response element-binding protein activity was reduced in these animals. Cumulatively, these data identify LRH-1 as a key regulatory component of the hepatic glucose-sensing system required for proper integration of postprandial glucose and lipid metabolism.

Introduction

The liver plays a central role in metabolic homeostasis by coordinating the synthesis, storage, breakdown, and redistribution of nutrients. Adequate control of these metabolic processes is of importance to accommodate systemic fuel requirements and availability. This is achieved through regulatory complexes that modulate both the catalytic activity and the expression level of metabolic enzymes. While the first usually enables rapid changes in enzymatic activity triggered by allosteric regulation or covalent modification, the second regulatory process is slower and involves transcription factors that adjust gene expression levels. In this context, nuclear receptors and their coregulators have been shown to play a key role in the transcriptional regulation of metabolic enzyme expression in response to changes in cellular nutrient and energy status (1, 2).

Liver receptor homolog 1 (LRH-1, also known as NR5A2), a member of the NR5A superfamily of nuclear receptors, is highly expressed in the liver. Hepatic LRH-1 promotes the expression of the bile acid–synthesizing enzymes *Cyp7a1* and *Cyp8b1* (3–5), while it suppresses acute phase response genes (6, 7). As a consequence, bile acid metabolism is altered in liver-specific LRH-1 knockout mice (3, 4), and LRH-1 heterozygous animals show an exacerbated inflammatory response (6). Other established LRH-1 target genes in the liver are known mediators of hepatic cholesterol uptake and efflux (8, 9), HDL formation (10, 11), cholesterol exchange between lipoproteins (12), and fatty acid synthesis (13). Although these findings point to a broader role for LRH-1 in hepatic lipid metabolism and reverse cholesterol transport, their physiological impact is as yet unknown.

Independent studies have demonstrated that human LRH-1 can bind several phospholipid species, including phosphoinositides (14–17). Interestingly, dilauroyl phosphatidylcholine (DLPC), which has been identified as a ligand for both mouse and human LRH-1 in vitro, was recently shown to confer LRH-1–dependent protection against hepatic steatosis and insulin resistance in mice exposed to chronic high-fat feeding (18). While these observations suggest that hepatic LRH-1 may contribute to metabolic control, the role of LRH-1 in hepatic glucose metabolism remains largely unexplored. However, insights into the mechanisms by which LRH-1 impacts on glucose and fatty acid metabolism in the liver are required for the development of therapeutic strategies to prevent or treat hepatic steatosis.

In this study, we assessed the physiological role of LRH-1 in hepatic intermediary metabolism. We show that LRH-1 controls the first step of hepatic glucose uptake through direct transcriptional regulation of the glucokinase (*Gck*) gene. As a result, mice lacking LRH-1 in hepatocytes fail to adequately induce glucose-driven glycolysis, glycogen synthesis, and fatty acid synthesis in the liver. Altogether, our work identifies LRH-1 as a critical regulatory component of the glucose-sensing system that integrates hepatic postprandial glucose and lipid metabolism.

Results

Reduced glucokinase and glycogen synthase fluxes in Alb-Cre;Lrh1$^{fl/fl}$ mice. To explore the putative involvement of LRH-1 in intermediary metabolism in the liver, we quantified hepatic glucose fluxes upon stable isotope infusion in mice with a somatic deletion of LRH-1 in hepatocytes (*Alb-Cre;Lrh1$^{fl/fl}$* mice; ref. 3) and their wild-type littermates (*Lrh1$^{fl/fl}$* mice) (Figure 1A; ref. 19). Blood glucose concentrations were similar in *Lrh1$^{fl/fl}$* and *Alb-Cre;Lrh1$^{fl/fl}$* mice under both normoglycemic and clamped hyperglycemic conditions (Table 1).

Conflict of interest: The authors have declared that no conflict of interest exists.
Citation for this article: *J Clin Invest.* 2012;122(8):2817–2826. doi:10.1172/JCI62368.

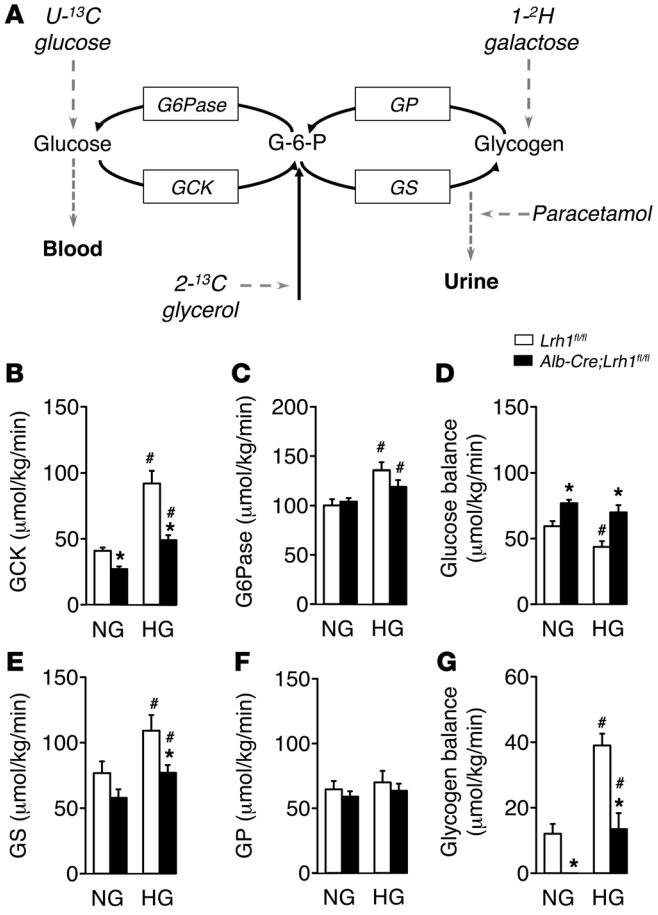

Figure 1
Reduced hepatic glucokinase and glycogen synthase fluxes in *Alb-Cre;Lrh1*$^{fl/fl}$ mice. (**A**) Schematic representation of the model used for mass isotopomer distribution analysis. GP, glycogen phosphorylase; GS, glycogen synthase; G6Pase, glucose-6-phosphatase. (**B**–**D**) Glucose fluxes in *Lrh1*$^{fl/fl}$ mice (white bars) and *Alb-Cre;Lrh1*$^{fl/fl}$ mice (black bars) under normoglycemic (NG) and hyperglycemic (HG) conditions. (**B**) Glucokinase and (**C**) glucose-6-phosphatase flux and (**D**) glucose balance. (**E**–**G**) Glycogen fluxes in *Alb-Cre;Lrh1*$^{fl/fl}$ and *Lrh1*$^{fl/fl}$ mice under normoglycemic and hyperglycemic conditions. (**E**) Glycogen synthase and (**F**) glycogen phosphorylase flux and (**G**) glycogen balance. Data represent mean ± SEM for n = 5–9 per genotype. $^{*}P < 0.05$ *Alb-Cre;Lrh1*$^{fl/fl}$ versus *Lrh1*$^{fl/fl}$; $^{\#}P < 0.05$ hyperglycemic versus normoglycemic.

Alb-Cre;Lrh1$^{fl/fl}$ mice showed significant reductions in the flux through glucokinase under both normoglycemic and hyperglycemic conditions (Figure 1B). In contrast, the glucose-6-phosphatase flux remained unaltered (Figure 1C), resulting in increased net glucose flux to the blood in *Alb-Cre;Lrh1*$^{fl/fl}$ mice (Figure 1D).

Hepatic LRH-1 deficiency also affected the conversion of glucose-6-phosphate (G6P) into glycogen. Normoglycemic and hyperglycemic glycogen synthase fluxes were lowered in *Alb-Cre;Lrh1*$^{fl/fl}$ mice (Figure 1E), while glycogen phosphorylase fluxes remained unchanged (Figure 1F). As a consequence, hepatic glycogen balances were markedly reduced in *Alb-Cre;Lrh1*$^{fl/fl}$ mice under both conditions (Figure 1G). Overall, hepatic ablation of LRH-1 reduced glucose phosphorylation via glucokinase and impaired the capacity of the liver to convert G6P into glycogen. Of interest, the whole-body glucose clearance rate was increased in *Alb-Cre;Lrh1*$^{fl/fl}$ mice under hyperglycemic conditions, presumably as a consequence of elevated insulin levels (Table 1). *Alb-Cre;Lrh1*$^{fl/fl}$ mice therefore required higher glucose infusion rates to maintain hyperglycemic states similar to those of their wild-type littermates (Table 1). However, these changes did not impact systemic energy metabolism. *Alb-Cre;Lrh1*$^{fl/fl}$ mice showed normal lean and fat masses, and food and water intake was unchanged compared with that of *Lrh1*$^{fl/fl}$ mice (Supplemental Figure 1, A and B; supplemental material available online with this article; doi:10.1172/JCI62368DS1). Energy expenditure and substrate utilization were also similar to those of wild-type controls (Supplemental Figure 1, C and D).

Glucokinase is a transcriptional target of LRH-1. To establish the basis of the reduced glucose fluxes, we evaluated the acute hepatic response to a glucose bolus in *Lrh1*$^{fl/fl}$ and *Alb-Cre;Lrh1*$^{fl/fl}$ mice. Glucose and insulin levels showed the expected increases (Figure 2, A and B) and were not affected in *Alb-Cre;Lrh1*$^{fl/fl}$ mice. The expression of *Lrh1* and its established target and corepressor SHP (20) was undetectable in *Alb-Cre;Lrh1*$^{fl/fl}$ mice (Figure 2C). Interestingly, the mRNA level of *Gck*, but not *Hk1*, was consistently reduced in the livers of *Alb-Cre;Lrh1*$^{fl/fl}$ mice, and its glucose-mediated increase was markedly blunted as compared with that in *Lrh1*$^{fl/fl}$ mice (Figure 2D). To evaluate whether the impaired induction of *Gck* in response to acute glucose availability also occurred upon prolonged glucose exposure, *Lrh1*$^{fl/fl}$ and *Alb-Cre;Lrh1*$^{fl/fl}$ mice were analyzed under fed, fasted, and refed conditions. Circulating glucose and insulin levels were similar between genotypes in the fed and fasted states but significantly increased in refed *Alb-Cre;Lrh1*$^{fl/fl}$ mice (Table 2). This was associated with lower pancreatic insulin content (Supplemental Figure 2), suggesting compensatory pancreatic insulin release as a result of impaired GCK-mediated hepatic glucose uptake in refed *Alb-Cre;Lrh1*$^{fl/fl}$ mice. As with *Lrh1* and its targets *Shp* and *Cyp8b1* (Figure 2E), the hepatic mRNA levels of *Gck* were robustly reduced in *Alb-Cre;Lrh1*$^{fl/fl}$ mice in all nutritional states (Figure 2F). *Hk1* expression remained unaffected by genotype or nutritional status (Figure 2F). Transient transfection assays revealed that LRH-1 contributes to basal *Gck* transcription irrespective of glucose

Table 1
Metabolic parameters during stable isotope infusion in *Lrh1*$^{fl/fl}$ and *Alb-Cre;Lrh1*$^{fl/fl}$ mice

	Normoglycemic		Hyperglycemic	
	Lrh1$^{fl/fl}$	*Alb-Cre;Lrh1*$^{fl/fl}$	*Lrh1*$^{fl/fl}$	*Alb-Cre;Lrh1*$^{fl/fl}$
Blood glucose (mmol/l)	7.2 ± 0.3	7.4 ± 0.3	17.0 ± 0.9^{A}	15.9 ± 0.7^{A}
Glucose clearance rate (ml/kg/min)	10.2 ± 0.5	11.5 ± 0.8	15.4 ± 0.9^{A}	19.9 ± 1.7^{A,B}
Plasma insulin (ng/ml)	ND	ND	0.2 ± 0.0	0.4 ± 0.1^{B}
Glucose infusion rate (μmol/kg/min)	4 ± 0	4 ± 0	258 ± 16^{A}	319 ± 45^{A}

ND, not determined. Data represent mean ± SEM for n = 5–9. $^{A}P < 0.05$ versus normoglycemic; $^{B}P < 0.05$ versus *Lrh1*$^{fl/fl}$.

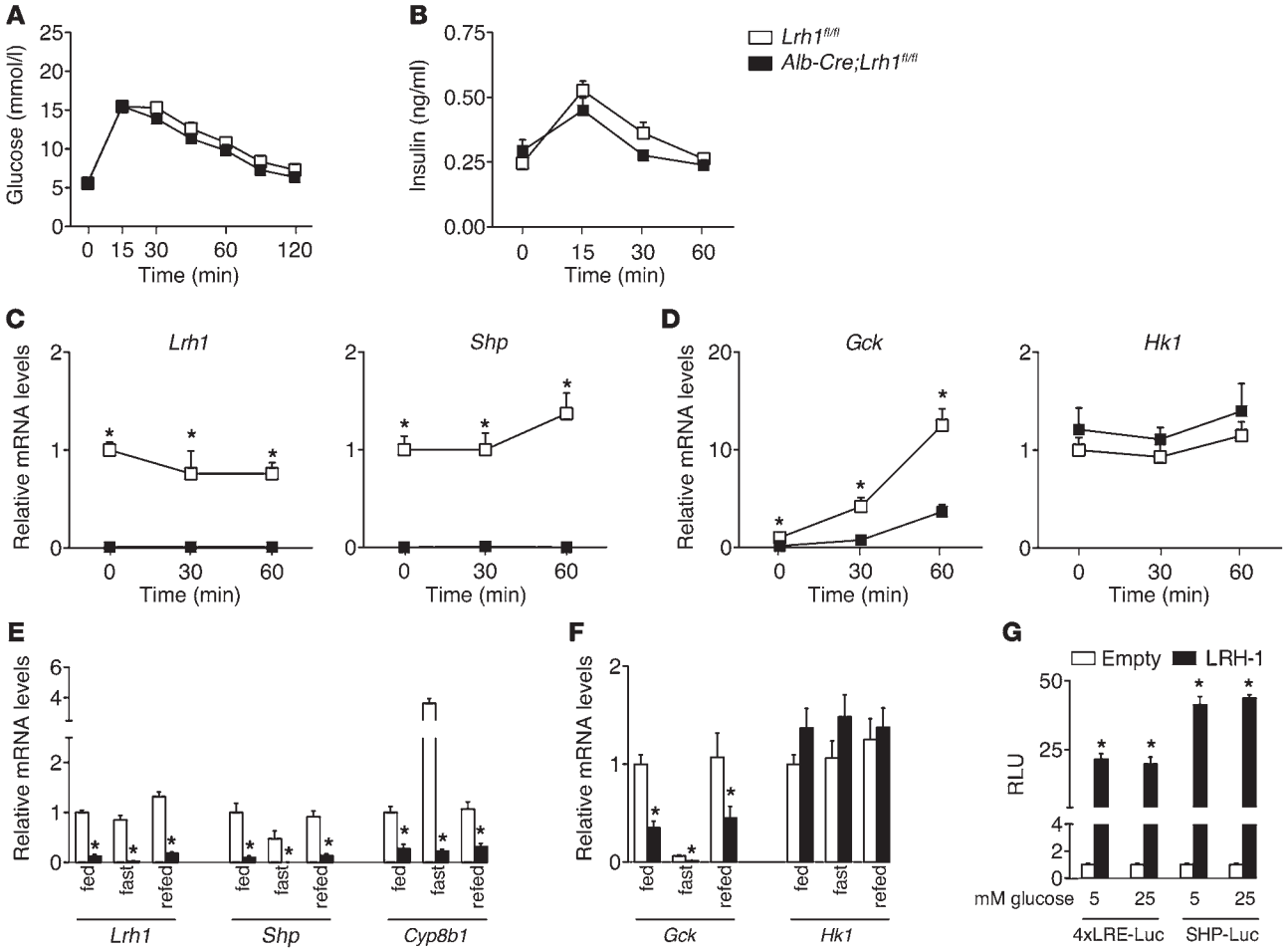

Figure 2

Reduced glucokinase expression in *Alb-Cre;Lrh1*$^{fl/fl}$ mice. (**A**) Blood glucose and (**B**) plasma insulin concentrations (n = 10 per genotype) and (**C** and **D**) hepatic mRNA levels of *Lrh1*, *Shp*, *Gck*, and *Hk1* during an oral glucose tolerance test (n = 4–8 per genotype) in *Lrh1*$^{fl/fl}$ mice (white boxes) and *Alb-Cre;Lrh1*$^{fl/fl}$ mice (black boxes). (**E** and **F**) Hepatic mRNA levels in fed, 24-hour–fasted or 6-hour–refed *Lrh1*$^{fl/fl}$ mice (white bars) and *Alb-Cre;Lrh1*$^{fl/fl}$ mice (black bars) (n = 7–9 per genotype). (**G**) LRH-1 transcriptional activity in HeLa cells transfected with a heterologous (4x LRH-1 response element–Luc [4xLRE-Luc]) or an endogenous LRH-1 reporter driven by the *Shp* promoter (SHP-Luc). Luciferase activity was determined in the absence (empty; white bars) or presence (LRH-1; black bars) of LRH-1 after exposure to 5 or 25 mM glucose for 24 hours. Data are expressed as relative light units (RLUs) compared with empty reporter (pGL3). Data represent mean ± SEM. *P < 0.05 versus *Lrh1*$^{fl/fl}$ or versus empty vector (pCMX).

availability, since activation of a heterologous and an endogenous LRH-1 reporter construct by LRH-1 was similar under low (5 mM) and high (25 mM) levels of glucose (Figure 2G).

We then evaluated whether glucokinase is subject to direct transcriptional control by LRH-1. Since *Lrh1* and *Shp* expression was abolished in the livers of *Alb-Cre;Lrh1*$^{fl/fl}$ mice (Figure 2, C and E), we first assessed whether changes in *Gck* mRNA levels arise from altered LRH-1 or SHP activity by means of adeno-associated viral vector-serotype 8–mediated (AAV8-mediated) SHP reconstitution in *Alb-Cre;Lrh1*$^{fl/fl}$ mice. Consistent with the lower expression of LRH-1 targets *Cyp8b1* and *Srb1*, SHP reconstitution also did not normalize the expression of *Gck* (Figure 3A). Reduced *Gck* mRNA levels in *Alb-Cre;Lrh1*$^{fl/fl}$ mice translated into lower GCK protein expression (Figure 3B). The LRH-1–mediated control of *Gck* expression was also confirmed in vitro. In line with reduced *Gck* mRNA levels in the absence of LRH-1, adenoviral overexpression of LRH-1 in mouse primary hepatocytes markedly induced *Lrh1*, *Shp*, *Cyp8b1*, and *Gck* expression (Figure 3C). Moreover, *Shp* and *Gck* mRNA levels were robustly elevated in mouse hepatoma cells that overexpressed LRH-1 (Figure 3D), resulting in enhanced glucose uptake and phosphorylation (Figure 3E). Computational analysis revealed 6 putative LRH-1 binding sites in the mouse *Gck* promoter (Figure 3F), and ChIP analysis of hepatic DNA from *Lrh1*$^{fl/fl}$ and *Alb-Cre;Lrh1*$^{fl/fl}$ mice identified specific recruitment of LRH-1 to sites 5 and 6, which are most proximal to the transcription initiation site in the hepatic *Gck* promoter (ref. 21; Figure 3, F and G). Site-directed mutagenesis of these sites identified site 6 downstream from the transcription initiation site as the major functional site that confers LRH-1 responsiveness (Figure 3H).

Reduced glycogen synthesis, glycolysis, de novo lipogenesis, and Chrebp activity in Alb-Cre;Lrh1$^{fl/fl}$ *mice*. Perturbed glucokinase activity impacts on hepatic glucose and lipid metabolism (22, 23). We

Table 2
Metabolite concentrations in fed, 24-hour–fasted, and 6-hour–refed *Lrh1*$^{fl/fl}$ and *Alb-Cre;Lrh1*$^{fl/fl}$ mice

	Fed		Fasted		Refed	
	Lrh1$^{fl/fl}$	*Alb-Cre;Lrh1*$^{fl/fl}$	*Lrh1*$^{fl/fl}$	*Alb-Cre;Lrh1*$^{fl/fl}$	*Lrh1*$^{fl/fl}$	*Alb-Cre;Lrh1*$^{fl/fl}$
Blood glucose (mmol/l)	7.6 ± 0.2	7.9 ± 0.3	3.9 ± 0.1^{A}	3.5 ± 0.2^{A}	7.6 ± 0.2^{B}	8.4 ± 0.3^{B,C}
Plasma insulin (ng/ml)	0.5 ± 0.1	0.5 ± 0.1	0.1 ± 0.0^{A}	0.1 ± 0.0^{A}	0.7 ± 0.1^{A,B}	1.2 ± 0.2^{A,B,C}
Plasma triglyceride (mmol/l)	1.2 ± 0.2	0.7 ± 0.1	1.1 ± 0.2	1.3 ± 0.1^{A}	1.4 ± 0.1^{B}	0.6 ± 0.1^{B,C}

Data represent mean ± SEM for n = 5–9. $^{A}P < 0.05$ versus fed; $^{B}P < 0.05$ versus fasted; $^{C}P < 0.05$ versus *Lrh1*$^{fl/fl}$.

hypothesized that hepatic ablation of LRH-1 would limit the availability of G6P for glycogen synthesis, glycolysis, and de novo lipogenesis. We therefore analyzed these biochemical pathways downstream of glucokinase in *Alb-Cre;Lrh1*$^{fl/fl}$ mice. In accordance with the reduction in the flux to glycogen (Figure 1, E and G), we observed that the accumulation of hepatic glycogen, which usually occurs within 30 minutes after an oral glucose bolus in *Lrh1*$^{fl/fl}$ mice, was markedly delayed in *Alb-Cre;Lrh1*$^{fl/fl}$ mice, in which glycogen levels were maximally increased after only 1 hour (Figure 4, A and B). In addition to this acute effect, glycogen content was also significantly lower in the livers of fed and refed *Alb-Cre;Lrh1*$^{fl/fl}$ mice (Figure 4C). In parallel to the reduced glucokinase flux in *Alb-Cre;Lrh1*$^{fl/fl}$ mice, we observed that primary hepatocytes from *Alb-Cre;Lrh1*$^{fl/fl}$ mice exhibited lower extracellular acidification rates when exposed to glucose, which is indicative of reduced glycolysis (Figure 4D). Besides its role in ATP generation, glycolysis also provides substrates for de novo fatty acid synthesis. Correspondingly, we found that gene expression of lipogenic enzymes was reduced in *Alb-Cre;Lrh1*$^{fl/fl}$ mice (Figure 5A). The induction of *Acaca* expression upon refeeding was attenuated in *Alb-Cre;Lrh1*$^{fl/fl}$ mice, while *Fasn* and *Scd1* mRNA levels were lower in all conditions studied (Figure 5A). *Acacb* expression was also reduced in refed *Alb-Cre;Lrh1*$^{fl/fl}$ mice (Figure 5A). To unequivocally establish the physiological relevance of these findings, we used ^{13}C-acetate to enrich the acetyl-CoA pool and quantified fractional de novo palmitate, stearate, and oleate synthesis rates (Figure 5B). Consistent with the reduction in glycolysis, de novo lipogenesis was reduced in fed and refed *Alb-Cre;Lrh1*$^{fl/fl}$ mice as compared with that in wild-type littermates (Figure 5B). Accordingly, plasma triglyceride concentrations were decreased in fed and refed *Alb-Cre;Lrh1*$^{fl/fl}$ mice compared with those in *Lrh1*$^{fl/fl}$ mice (Table 2).

Previous work has shown that hepatic GCK ablation reduces carbohydrate response element-binding protein (*Chrebp*) and pyruvate kinase (*Pklr*) expression (23). In accordance with this, and consistent with the observed reduction in glycolysis (Figure 4D) and de novo lipogenesis (Figure 5), we observed that the expression of *Chrebp* and *Pklr* was lower in fed and refed *Alb-Cre;Lrh1*$^{fl/fl}$ mice (Figure 6A). On the other hand, the mRNA levels of sterol regulatory element binding protein 1c (*Srebp-1c*) and its target gene glucose-6-phosphate dehydrogenase (*G6pd1*) were not changed in *Alb-Cre;Lrh1*$^{fl/fl}$ mice (Figure 6A). Nuclear ChREBP protein was also reduced in refed *Alb-Cre;Lrh1*$^{fl/fl}$ mice (Figure 6B), consistent with lower hepatic G6P content under these conditions (Figure 6C; ref. 24). This was not attributed to the concomitant loss of hepatic SHP in the *Alb-Cre;Lrh1*$^{fl/fl}$ mice, since *Shp* reconstitution did not restore *Chrebp* and *Pklr* mRNA levels (Figure 6D). To establish whether the reduction in glycolytic and lipogenic gene expression in the livers of *Alb-Cre;Lrh1*$^{fl/fl}$ mice results from direct regulation of *Chrebp* transcription by LHR-1, we evaluated the effect of LRH-1 on *Chrebp* promoter activation. Unlike the *Gck* promoter (Figure 3H), LRH-1 did not directly activate the mouse *Chrebp* promoter, while a robust transactivation of the *Shp* promoter was observed in response to LRH-1 (Figure 6E), indicating that LRH-1 impacts ChREBP in an indirect manner.

Based on previous studies showing that GCK is required for optimal ChREBP expression and activity (23–25), we postulated that LRH-1 indirectly modulates ChREBP via GCK. To support this hypothesis, we rescued hepatic *Gck* expression in *Alb-Cre;Lrh1*$^{fl/fl}$ mice by AAV8-mediated gene transfer (Figure 6F). Consistent with reduced nuclear ChREBP expression and hepatic G6P content (Figure 6, B and C), *Pklr* and *Acaca* mRNA levels were normalized in *Alb-Cre;Lrh1*$^{fl/fl}$ mice upon *Gck* reconstitution, indicating that the lower expression levels of these ChREBP target genes occurs secondary to a reduced flux through GCK in *Alb-Cre;Lrh1*$^{fl/fl}$ mice. Hepatic *Fasn* expression, on the other hand, remained low upon GCK reconstitution in *Alb-Cre;Lrh1*$^{fl/fl}$ mice, consistent with a previous study that identified this gene as a direct target of LRH-1 (13). *Scd1* mRNA levels showed a dose-dependent response to *Gck* rescue in *Alb-Cre;Lrh1*$^{fl/fl}$ mice (Figure 6F). Combined, these data indicate that LRH-1 acts as an upstream regulator of GCK and as such indirectly impacts glycolytic and, at least in part, lipogenic gene expression.

Discussion

Hepatic LRH-1 is an established transcriptional regulator of cholesterol and bile acid homeostasis (3–5, 14, 26). Here, we report that LRH-1 directly regulates intrahepatic glucose and fatty acid metabolism during the postprandial phase. Our data show that both loss and gain of LRH-1 function control glucokinase expression and impact hepatic glucose uptake in liver and hepatocytes. The LRH-1–driven flux through glucokinase in turn critically determines the partitioning of G6P toward glycogen storage, glycolysis, and de novo lipogenesis. Hence, we believe that this study confirms the unique and essential ability of hepatic glucokinase to properly accommodate glucose availability to its oxidation and storage (22, 23, 27) and reveals a novel upstream regulator of its activity that determines the capacity for hepatic glucose uptake upon glucose exposure.

Glucokinase mediates hepatic glucose uptake and, as such, represents the first step of glucose metabolism in the liver. Its product, G6P, is a central metabolite for intrahepatic glucose and lipid homeostasis. This metabolite serves as the substrate for the oxidation of glucose as well as its storage as glycogen and fat. Hepatic glucokinase expression depends on the nutritional state and is subject to reciprocal regulation by insulin and glucagon (28). Different transcription factors, including liver X receptor (LXR), PPARγ, and SREBP-1c, are known to interact to control glucokinase

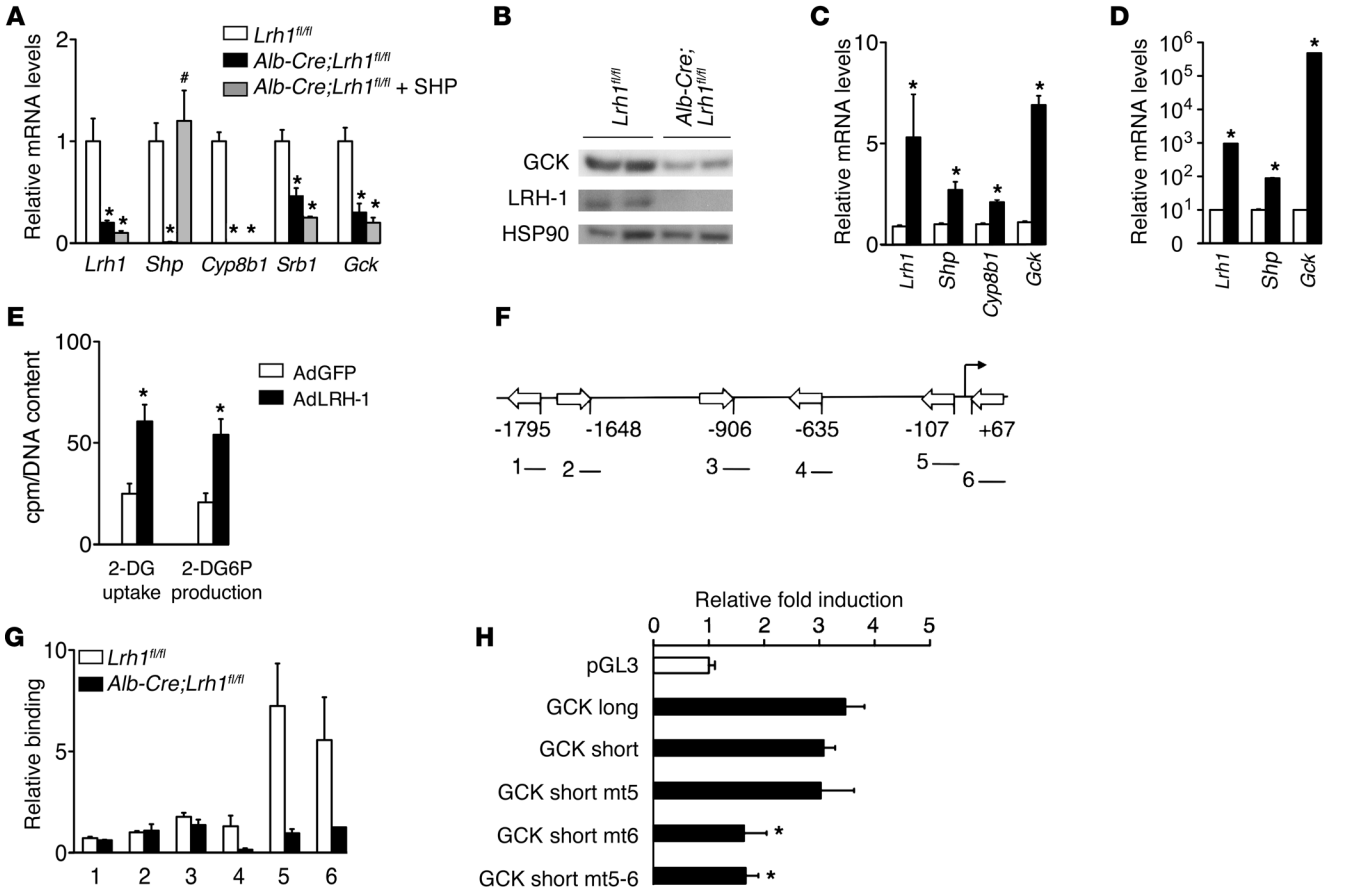

Figure 3

Gck is a direct transcriptional target of LRH-1. (**A**) Hepatic mRNA levels in *Alb-Cre;Lrh1*$^{fl/fl}$ mice 5 weeks after in vivo transduction of the liver using AAV8-SHP virus (gray bars) in comparison with those in *Lrh1*$^{fl/fl}$ mice (white bars) and *Alb-Cre;Lrh1*$^{fl/fl}$ mice (black bars) (n = 4–5 per group). (**B**) Hepatic GCK protein expression in refed *Lrh1*$^{fl/fl}$ and *Alb-Cre;Lrh1*$^{fl/fl}$ mice. (**C** and **D**) Expression levels of LRH-1 and its targets in (**C**) wild-type primary hepatocytes and (**D**) Hepa 1.6 mouse hepatoma cells transduced with AdGFP (white bars) or AdLRH-1 (black bars) viruses (n = 3 per condition). (**E**) 2-deoxyglucose (2-DG) uptake and 2-deoxyglucose-6-phosphate (2-DG6P) production in Hepa 1.6 cells transduced with AdGFP (white bars) or AdLRH-1 (black bars) viruses (n = 6 per condition). (**F**) Schematic presentation of the 6 putative LRH-1 response elements in the mouse *Gck* promoter. (**G**) Assessment of LRH-1 recruitment to these sites, as depicted in **F**, determined by ChIP analysis using genomic DNA from livers of *Lrh1*$^{fl/fl}$ and *Alb-Cre;Lrh1*$^{fl/fl}$ mice. (**H**) Luciferase activities in HeLa cells transfected with empty luciferase reporter (pGL3; white bar) or long and short *Gck* promoter constructs (black bars). Data are expressed as fold induction in luciferase activity upon LRH-1 cotransfection. Data represent mean ± SEM. *P < 0.05 versus *Lrh1*$^{fl/fl}$, versus GFP, or versus empty reporter (pGL3); #P < 0.05 versus *Alb-Cre;Lrh1*$^{fl/fl}$.

expression (29). The induction of *Gck* in response to refeeding is, however, not significantly impaired in *LXR*- or *Srebp-1c*–deficient mice (30–32). In this study, we observed a profound and consistent reduction in *Gck* mRNA levels in fed, fasted, and refed *Alb-Cre;Lrh1*$^{fl/fl}$ mice, confirming previous observations in insulin-resistant mice (18). Together, these data suggest that LRH-1 is a major regulator of hepatic glucokinase expression. Metabolic alterations in *Alb-Cre;Lrh1*$^{fl/fl}$ mice may, however, also be related to lower *Shp* expression. This is of importance given that SHP acts as a transrepressor on LXRα- or PPARγ-mediated *Gck* induction (29). However, a recent report showed that SHP deficiency does not impact hepatic *Gck* expression in chow-fed mice (33). This observation is consistent with the results obtained in this study. By means of ChIP analysis, site-directed mutagenesis, and SHP reconstitution experiments, we have firmly established that LRH-1 directly controls *Gck* transcription.

LRH-1 specifically acts on glucokinase transcription, since no significant differences in hexokinase expression were observed between *Lrh1*$^{fl/fl}$ and *Alb-Cre;Lrh1*$^{fl/fl}$ mice. This is of particular interest, because it has been shown that only G6P generated through glucokinase determines the metabolic fate of intrahepatic glucose (34, 35). Liver-specific glucokinase knockout mice show a reduction in glycogen synthesis under hyperglycemic conditions (22). In this study, we also observed reduced glycogen storage and a lower glycogen synthase flux in the livers of *Alb-Cre;Lrh1*$^{fl/fl}$ mice. Glucokinase is furthermore required to increase *Chrebp* mRNA levels in response to refeeding and is critical for the ChREBP-mediated induction of glycolytic and lipogenic genes in response to glucose (23). Importantly, recent work has identified G6P as the actual metabolic signal that drives ChREBP-mediated control of glycolysis and lipogenesis (24, 25). In line with this, we observed that refed *Alb-Cre;Lrh1*$^{fl/fl}$ mice showed reduced hepatic G6P content along

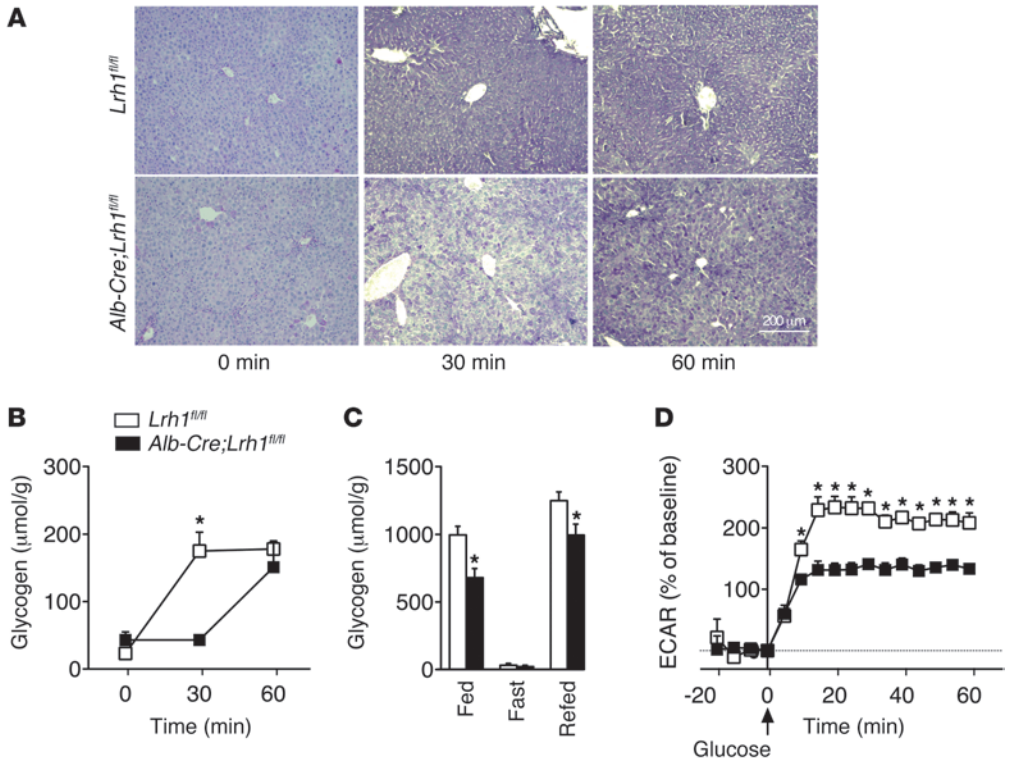

Figure 4
Delayed glycogen synthesis and reduced glycolysis in *Alb-Cre;Lrh1*$^{fl/fl}$ mice. (**A**) Representative glycogen stainings during oral glucose tolerance test (n = 3–8 per genotype). Scale bar: 200 μm. (**B**) Quantification of hepatic glycogen content in *Lrh1*$^{fl/fl}$ mice (white boxes) and *Alb-Cre;Lrh1*$^{fl/fl}$ mice (black boxes) during oral glucose tolerance test. (**C**) Hepatic glycogen content in fed, 24-hour–fasted, or 6-hour–refed *Lrh1*$^{fl/fl}$ mice (white bars) and *Alb-Cre;Lrh1*$^{fl/fl}$ mice (black bars) (n = 7 per genotype). (**D**) Extracellular acidification rates (ECARs) in *Lrh1*$^{fl/fl}$ (white boxes) and *Alb-Cre;Lrh1*$^{fl/fl}$ (black boxes) primary hepatocytes (n = 5–6 per genotype). Data represent mean ± SEM. *P < 0.05 versus *Lrh1*$^{fl/fl}$.

with a suboptimal induction of glycolytic and lipogenic genes. The reconstitution of hepatic SHP furthermore revealed that, similar to those of *Gck*, the lower expression levels of *Chrebp* and its target *Pklr* in *Alb-Cre;Lrh1*$^{fl/fl}$ mice are also caused by the absence of LRH-1, and not SHP, in the liver. Reduced mRNA levels of *Chrebp* and its targets in *Alb-Cre;Lrh1*$^{fl/fl}$ mice were associated with lowered glycolytic and lipogenic fluxes as well as reduced plasma triglyceride levels. The reduction in glycolysis in *Alb-Cre;Lrh1*$^{fl/fl}$ mice results from impaired GCK activity, as *Pklr* expression was completely normalized upon hepatic *Gck* rescue. *Gck* reconstitution also restored the mRNA levels of the ChREBP target *Acaca*, but not the expression of *Fasn*, which is a direct target of both ChREBP and LRH-1 (13, 23). The reduced de novo lipogenesis in *Alb-Cre;Lrh1*$^{fl/fl}$ mice therefore most likely results from a concerted impairment of both ChREBP-dependent and LRH-1–dependent lipogenesis. Thus, although the flux through glucokinase is only partially inhibited in *Alb-Cre;Lrh1*$^{fl/fl}$ mice, these animals present a striking phenotypic resemblance to liver-specific glucokinase knockout mice with regard to glycogen storage and ChREBP-mediated glycolysis and lipogenesis (22, 23).

Genetic models of obesity and type 2 diabetes, including *ob/ob* and *db/db* mice, have been reported to display increased hepatic glucokinase expression and flux (36–38), along with ChREBP hyperactivity and hepatic steatosis, which is partially reversible by ChREBP inhibition (39). Importantly, glucokinase expression is also associated with lipogenic activity and fatty liver in humans (40). This implies that a reduction in LRH-1 activity would have a potential protective effect on steatosis development via reduced glucokinase-mediated ChREBP activation when hepatic glucose availability is high, e.g., in obese diabetic states. Although *Alb-Cre;Lrh1*$^{fl/fl}$ mice are not protected against high-fat diet–induced glucose intolerance and insulin resistance (Supplemental Figure 3 and ref. 18), it was recently shown that DLPC administration improves insulin sensitivity and liver steatosis in an LRH-1–dependent manner (18). It was proposed that DLPC-mediated LRH-1 activation interferes with the insulin/SREBP-1c signaling cascade that drives lipogenesis in the liver. In this study, we observed that the hepatic mRNA levels of *Srebp-1c* and its target *G6pd1* were unaltered in insulin-sensitive *Alb-Cre;Lrh1*$^{fl/fl}$ mice. This is in agreement with a report showing that *Srebp-1c* and *G6pd1* expression levels are not altered upon glucokinase overexpression, while those of the ChREBP targets *Pklr* and *Acaca/Acacb* are induced (41). Combined, current and previous findings (18) indicate that LRH-1 impacts on hepatic lipogenesis via alternate routes under different nutritional and pathophysiological conditions.

In conclusion, these data indicate that LRH-1 is a major and essential transcriptional regulator of glucokinase, the gatekeeper of hepatic glucose metabolism. As a consequence, LRH-1 not only controls the initial step of glucose uptake but also determines the intrahepatic fate of its product G6P. Our data identifies LRH-1 as a critical component of the hepatic glucose-sensing system that integrates glucose and lipid homeostasis in the postprandial phase.

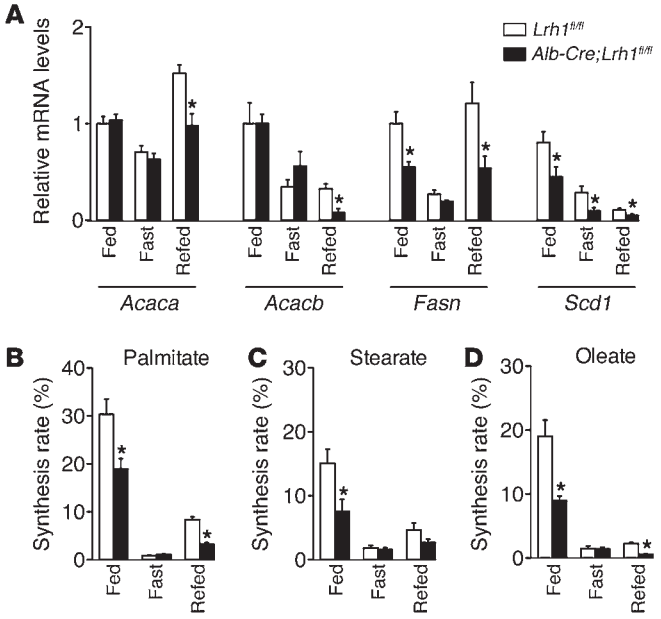

Figure 5
Reduced de novo lipogenesis in *Alb-Cre;Lrh1*$^{fl/fl}$ mice. (**A**) Hepatic lipogenic gene expression and (**B**) de novo synthesis of hepatic palmitate, stearate, and oleate in fed, fasted, and refed *Lrh1*$^{fl/fl}$ mice (white bars) and *Alb-Cre;Lrh1*$^{fl/fl}$ mice (black bars) (n = 7–9 per genotype). Data represent mean ± SEM. *P < 0.05 versus *Lrh1*$^{fl/fl}$.

Methods

For more details, see the Supplemental Methods. Unless otherwise indicated, all chemical reagents were obtained from Sigma-Aldrich.

Generation of viral vectors. AAV8 encoding the mouse SHP or GCK cDNAs (AAV8-SHP or AAV8-GCK), driven by the hybrid cytomegalovirus enhancer/chicken β-actin constitutive promoter or the liver-specific α1-antitrypsin promoter (hAAT; ref. 42), respectively, were generated and titrated as described previously to enable their use in vivo (43, 44). Plasmids used to generate viral particles and the hAAT promoter were provided by K.A. High, Children's Hospital of Philadelphia, Philadelphia, Pennsylvania, USA. For in vitro experiments, cells were transduced with an adenoviral vector encoding the mouse *Lrh1* gene (AdLRH-1; derived from pCMX-mLRH-1; ref. 8) using the Adeno-X Expression System (Clontech).

Animal studies. LRH-1 floxed mice (3) were crossed with serum albumin-Cre mice (The Jackson Laboratory) and then further intercrossed to generate hepatocyte-specific LRH-1 knockout (*Alb-Cre;Lrh1*$^{fl/fl}$) and wild-type (*Lrh1*$^{fl/fl}$) mice on a pure C57BL/6J background. Animals had ad libitum access to regular chow (Teklad no. 2016, Harlan) and drinking water and were kept under a 12-hour-dark/12-hour-light cycle (lights on 7 AM to 7 PM). At the end of the experiments, mice were sacrificed by cardiac puncture under isoflurane anesthesia, and livers were quickly snap frozen.

For quantification of carbohydrate fluxes, mice were equipped with a permanent jugular vein catheter, after which they were allowed a recovery period of at least 3 days (45). Prior to the infusion experiment, mice were fasted overnight. They were infused with a solution containing [U-^{13}C]glucose, [2-^{13}C]glycerol, [1-^{2}H]galactose, and paracetamol at an infusion rate of 0.6 ml per hour, as previously described, for 210 minutes (19). Then, the infusion of a second solution containing glucose (1,067 mM) and [U-^{13}C]glucose (50 mM) was initiated, while the infusion of the first solution was continued. The infusion rate of the second solution was adjusted according to the blood glucose concentration in order to maintain comparable hyperglycemia in both genotypes. These infusions were prolonged for another 210 minutes. During the entire experiment, blood glucose concentrations were measured and blood and urine samples were collected on filter paper at regular time intervals (46). After 420 minutes, mice were sacrificed.

For oral glucose tolerance tests, mice were fasted overnight and subsequently challenged with a glucose bolus (2 g/kg) by gavage. At regular time points, blood glucose concentrations were measured, and blood samples were collected to determine insulin levels. Separate groups of mice were sacrificed after 0, 30, and 60 minutes.

For fasting-refeeding experiments, fed and 24-hour–fasted mice were sacrificed at 7 AM. Refed mice were fasted for 24 hours, starting at 7 AM, and were subsequently refed with normal chow diet for 6 hours. To quantify fatty acid synthesis rates, all mice received sodium[1-^{13}C] acetate via their drinking water (2%) 24 hours prior to sacrifice.

For SHP reconstitution experiments, *Alb-Cre;Lrh1*$^{fl/fl}$ mice received an injection of SHP-AAV8 vector (10^{12} particles per mouse) into the jugular vein under isoflurane anesthesia. Five weeks after vector administration, the mice were sacrificed after a 6-hour fast. For GCK reconstitution experiments, *Alb-Cre;Lrh1*$^{fl/fl}$ mice received an injection of GCK-AAV8 vector (10^{11} or 10^{12} particles per mouse) into the jugular vein under isoflurane anesthesia. Five weeks after vector administration, the mice were sacrificed after 6 hours of refeeding. Hepatic gene expression levels were compared with those of *Lrh1*$^{fl/fl}$ and *Alb-Cre;Lrh1*$^{fl/fl}$ mouse AAV8 vector particles carrying a noncoding genome (AAV8-null).

Biochemical analysis. The extraction of glucose from blood and urine spots, the derivatization of the extracted compounds, the GC-MS analysis of these derivatives, and the calculation of hepatic carbohydrate fluxes were performed as described previously (46, 47). Blood glucose concentrations were measured using a Maxi Kit glucometer (Bayer Diagnostics). Plasma insulin and triglyceride concentrations were determined using commercially available ELISA (Crystal Chem Inc.) and enzymatic kits (Roche), respectively. Hepatic triglyceride content was quantified after lipid extraction (48) using an enzymatic assay (Roche). Fatty acids derived from these hepatic lipid extracts were liberated, derivatized, and subjected to GC-MS analysis in order to calculate fractional synthesis rates from the incorporation of ^{13}C-acetate as described previously (49). Hepatic glycogen and G6P content were determined using enzymatic assays (50, 51).

Histological analysis. In order to visualize hepatic glycogen disposition, hematoxylin and eosin and periodic acid-Schiff stainings were performed on 4-μm-thick liver sections.

Cell culture. Primary hepatocytes were isolated using collagenase perfusion as described previously with minor modifications (23). Hepatocytes from *Lrh1*$^{fl/fl}$ mice were plated in DMEM 4.5 g/l glucose with 10% FBS. Four hours after plating, cells were transduced with AdLRH-1 or AdGFP. Hepatocytes were then incubated in DMEM 4.5 g/l glucose without serum for 36 hours and lysed for RNA isolation.

Primary hepatocytes from *Alb-Cre;Lrh1*$^{fl/fl}$ and *Lrh1*$^{fl/fl}$ mice were seeded in Seahorse XF24 plates (Seahorse Bioscience) containing glucose-free medium without serum for 24 hours. They were subsequently exposed to 25 mM glucose, and the extracellular acidification rate (a measure of glycolysis) was measured at 5-minute intervals by the Seahorse XF24 system (Seahorse Bioscience).

Hepa 1.6 mouse hepatoma cells were cultured in DMEM 4.5 g/l glucose with 10% FBS, 1% NEAA, and 0.1% gentamicin. These cells were transduced with AdLRH-1 or AdGFP. After 12 hours, media were changed and incubation was continued for another 30 hours. Then, cells were rinsed with PBS 3 times and either lysed in Tri Reagent (Invitrogen) for RNA isolation or exposed to 2-[^{14}C]deoxyglucose (DOG; 0.1 mCi) for 10 minutes to quantify DOG incorporation as described previously (52). In short, cells were rinsed with 0.1 mM phloretin to further inhibit sugar efflux

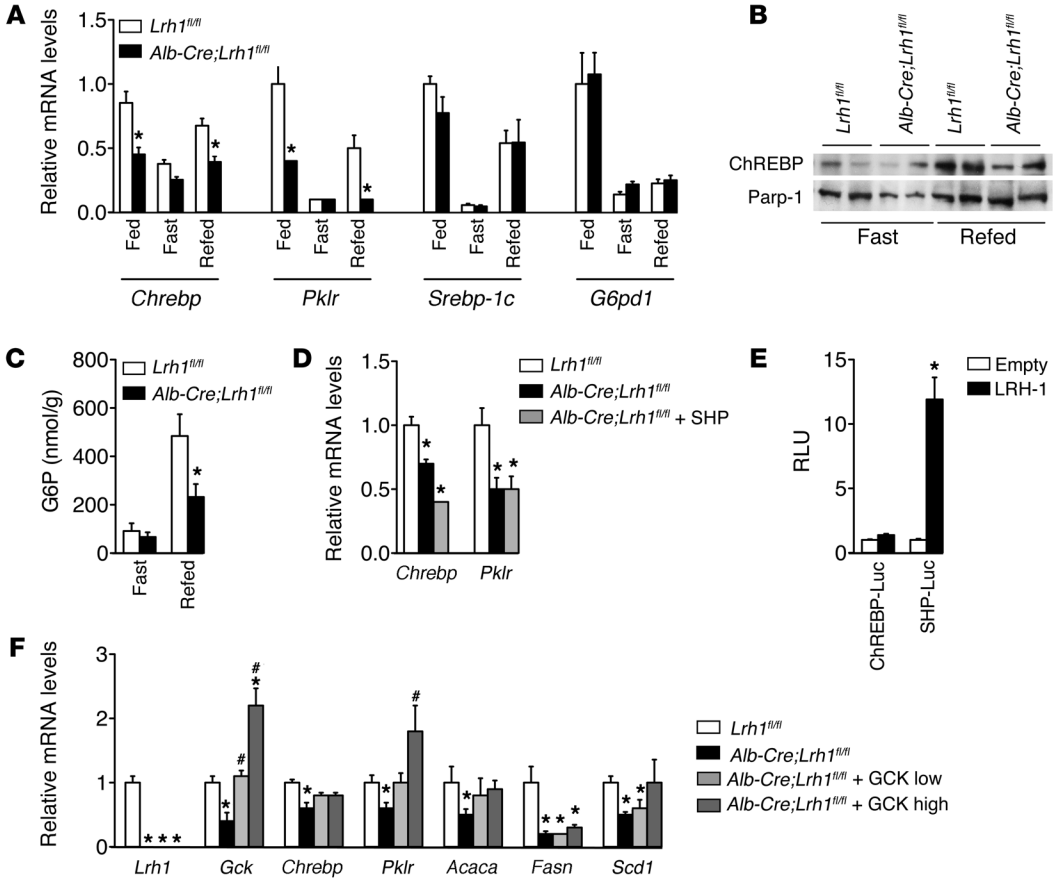

Figure 6

Impaired GCK activity in *Alb-Cre;Lrh1*$^{fl/fl}$ mice reduces ChREBP expression and activity. (**A**) Hepatic *Chrebp*, *Pklr*, *Srebp-1c*, and *G6pd1* expression in fed, 24-hour–fasted, or 6-hour–refed *Lrh1*$^{fl/fl}$ mice (white bars) and *Alb-Cre;Lrh1*$^{fl/fl}$ mice (black bars) (n = 7–9 per genotype). (**B**) Nuclear ChREBP protein expression in 24-hour–fasted and 6-hour–refed *Lrh1*$^{fl/fl}$ and *Alb-Cre;Lrh1*$^{fl/fl}$ mice. (**C**) Hepatic G6P content in fasted and refed *Lrh1*$^{fl/fl}$ mice (white bars) and *Alb-Cre;Lrh1*$^{fl/fl}$ mice (black bars) (n = 6–7 per genotype). (**D**) Hepatic *Chrebp* and *Pklr* expression in *Alb-Cre;Lrh1*$^{fl/fl}$ mice 5 weeks after in vivo transduction of the liver using AAV8-SHP virus (gray bars) in comparison with that in *Lrh1*$^{fl/fl}$ mice (white bars) and *Alb-Cre;Lrh1*$^{fl/fl}$ mice (black bars) (n = 4–5 per group). (**E**) Luciferase activities in HeLa cells transfected with *Chrebp* (ChREBP-Luc) or *SHP* (SHP-Luc) promoter (black bars) constructs in the absence (empty; white bars) or presence (LRH-1; black bars) of LRH-1. Data are expressed as relative light units and normalized to empty reporter (pGL3). (**F**) Hepatic mRNA levels in *Alb-Cre;Lrh1*$^{fl/fl}$ mice 5 weeks after in vivo transduction of the liver using 2 different titers of AAV8-GCK virus (low, 10^{11} particles per mouse [light gray bars], and high, 10^{12} particles per mouse [dark gray bars]) in comparison with those in *Lrh1*$^{fl/fl}$ mice (white bars) and *Alb-Cre;Lrh1*$^{fl/fl}$ mice (black bars) (n = 4–5 per group). Data represent mean ± SEM. *P < 0.05 versus *Lrh1*$^{fl/fl}$ or versus empty vector (pCMX); $^{\#}P$ < 0.05 versus *Alb-Cre;Lrh1*$^{fl/fl}$.

and lysed in 1 M NaOH at 60°C for 10 minutes. The lysates were neutralized in 1 M HCl and centrifuged. 0.3 M $ZnSO_4$ and 0.3 M $Ba(OH)_2$ were added to the supernatant, and the mixture was centrifuged. Then, 6% perchloric acid was added to the supernatant. After the centrifugation, the radioactivity of the supernatant was measured by a liquid scintillation counter. Radioactive counts were normalized to DNA content to determine DOG uptake and G6P production.

Cloning and site-directed mutagenesis. A 0.6-kb fragment (–601 to +10) of the murine *Shp* promoter, as well as a long (~1.2 kb; –1,063 to +141) and short (~0.6 kb; –514 to +141) fragment of the murine hepatic *Gck* promoter (21) (GCK long and short), were amplified from mouse liver genomic DNA. These fragments were inserted into the multiple cloning site of the pGL3-basic reporter (Promega Life Science). The heterologous LRH-1 reporter vector was generated by subcloning 4 repeats of an established LRH-1 response element in the human *Shp* promoter (–79 to –71) into the multiple cloning site of the TK-pGL3 reporter (Promega Life Science).

Mutations in putative LRH-1 responsive elements 5 and 6 (Figure 3F) in the GCK short reporter were introduced using the QuikChange Site-Directed Mutagenesis Kit (Stratagene). Additional mutagenesis was performed to obtain GCK short mutant elements 5 and 6 (mt5-6), from the GCK short mt5. The sequences of all reporter constructs were analyzed and confirmed.

Transient transfection and cell reporter assays. All transfections were performed using Lipofectamin 2000 (Invitrogen). HeLa cells were transfected under low (5 mM) glucose conditions with reporter constructs driven by a heterologous promoter, consisting of 4 consensus LRH-1 response elements, or driven by the endogenous *Shp* promoter in the presence of either pCMX-mLRH-1 or pCMX-empty (8). After 6 hours, media were changed to either high (25 mM) or low (5 mM) glucose. Luciferase activities were determined 24 hours later and normalized for β-galactosidase activities. Luciferase activities in HeLa cells transfected with *Chrebp* promoter reporter (53), the *Shp* promoter reporter, or the different *Gck* promoter reporters

in normal culture conditions (25 mM glucose) in the presence of either pCMX-mLRH-1 or pCMX-empty were determined 30 hours after transfection and normalized for β-galactosidase activities. All experiments were performed 3 times, and data represent average values of a representative experiment, which was performed in quadruplicate and normalized for empty luciferase reporter (pGL3) activity.

Quantitative RT-PCR and ChIP. RNA was isolated from liver samples and cells using Tri Reagent, and quantitative RT-PCR was performed as described previously (3). Primer sequences are listed in Supplemental Table 1. Gene expression levels were normalized for β_2 microglobulin.

ChIP analysis was performed as described previously with minor adaptations (54). DNA was purified using the PCR clean-up Gel extraction Kit (Macherey-Nagel), after which qPCR was performed as described previously (3). Data were normalized for GAPDH promoter binding and expressed relative to IgG. ChIP primer sequences are listed in Supplemental Table 1.

Western blot analysis. Total liver and nuclear protein extracts were prepared, and lysates were subjected to Western blotting as described previously (3). Blots were probed with GCK (55), ChREBP (Novus), LRH-1 (56), Parp-1 (Santa Cruz Biotechnology Inc.), and HSP90 (BD Transduction Laboratories).

Statistics. Data are presented as mean ± SEM. Statistical significance ($P < 0.05$) was assessed using the Kruskal-Wallis test followed by the Conover test for post-hoc analysis.

Study approval. All animal studies were performed in accordance with Swiss animal protection law and were approved by the Cantonal Veterinary Office (Vaud, Switzerland) and the local committee for animal experimentation (license no. 2331; Ecole Polytechnique Fédérale de Lausanne).

Acknowledgments

The authors thank Thibaud Clerc, Jiujiu Yu, Amandine Signorino-Gelo, Dongryeol Ryu, Pablo Fernandez-Marcos, Sabrina Bichet, Aycha Bleeker, Rick Havinga, and Niels Kloosterhuis for technical assistance and discussion. The ChREBP reporter was provided by K. Gauthier (Institut de Génomique Fonctionnelle de Lyon, Université de Lyon, Lyon, France). This work was supported by the Ecole Polytechnique Fédérale de Lausanne, the Swiss National Science Foundation, the Swiss Cancer League, and the FP7 programme EUGENE2. M.H. Oosterveer is supported by a fellowship from the Royal Netherlands Academy of Arts and Sciences. J. Auwerx is the Nestlé Chair in Energy Metabolism.

Received for publication December 9, 2011, and accepted in revised form May 30, 2012.

Address correspondence to: Kristina Schoonjans, Ecole Polytechnique Fédérale de Lausanne (EPFL), Laboratory of Integrative and Systems Physiology, NCEM, SV, IBI, AI1149, Station 15, CH-1015 Lausanne, Switzerland. Phone: 41.21.6931891; Fax: 41.21.6939600; E-mail: kristina.schoonjans@epfl.ch.

1. Feige JN, Auwerx J. Transcriptional coregulators in the control of energy homeostasis. *Trends Cell Biol*. 2007;17(6):292–301.
2. McKenna NJ, et al. Minireview: evolution of NURSA, the nuclear receptor signaling atlas. *Mol Endocrinol*. 2009;23(6):740–746.
3. Mataki C, et al. Compromised intestinal lipid absorption in mice with a liver-specific deficiency of liver receptor homolog 1. *Mol Cell Biol*. 2007;27(23):8330–8339.
4. Out C, et al. Liver receptor homolog-1 is critical for adequate up-regulation of Cyp7a1 gene transcription and bile salt synthesis during bile salt sequestration. *Hepatology*. 2011;53(6):2075–2085.
5. Lee YK, et al. Liver receptor homolog-1 regulates bile acid homeostasis but is not essential for feedback regulation of bile acid synthesis. *Mol Endocrinol*. 2008;22(6):1345–1356.
6. Venteclef N, Smith JC, Goodwin B, Delerive P. Liver receptor homolog 1 is a negative regulator of the hepatic acute-phase response. *Mol Cell Biol*. 2006;26(18):6799–6807.
7. Venteclef N, Delerive P. Interleukin-1 receptor antagonist induction as an additional mechanism for liver receptor homolog-1 to negatively regulate the hepatic acute phase response. *J Biol Chem*. 2007;282(7):4393–4399.
8. Schoonjans K, et al. Liver receptor homolog 1 controls the expression of the scavenger receptor class B type I. *EMBO Rep*. 2002;3(12):1181–1187.
9. Freeman LA, et al. The orphan nuclear receptor LRH-1 activates the ABCG5/ABCG8 intergenic promoter. *J Lipid Res*. 2004;45(7):1197–1206.
10. Delerive P, Galardi CM, Bisi JE, Nicodeme E, Goodwin B. Identification of liver receptor homolog-1 as a novel regulator of apolipoprotein AI gene transcription. *Mol Endocrinol*. 2004;18(10):2378–2387.
11. Venteclef N, Haroniti A, Tousaint JJ, Talianidis I, Delerive P. Regulation of anti-atherogenic apolipoprotein M gene expression by the orphan nuclear receptor LRH-1. *J Biol Chem*. 2008;283(7):3694–3701.
12. Luo Y, Liang CP, Tall AR. The orphan nuclear receptor LRH-1 potentiates the sterol-mediated induction of the human CETP gene by liver X receptor. *J Biol Chem*. 2001;276(27):24767–24773.
13. Matsukuma KE, Wang L, Bennett MK, Osborne TF. A key role for orphan nuclear receptor liver receptor homologue-1 in activation of fatty acid synthase promoter by liver X receptor. *J Biol Chem*. 2007;282(28):20164–20171.
14. Lee YK, Moore DD. Liver receptor homolog-1, an emerging metabolic modulator. *Front Biosci*. 2008;13:5950–5958.
15. Ingraham HA, Redinbo MR. Orphan nuclear receptors adopted by crystallography. *Curr Opin Struct Biol*. 2005;15(6):708–715.
16. Mullaney BC, et al. Regulation of C. elegans fat uptake and storage by acyl-CoA synthase-3 is dependent on NR5A family nuclear hormone receptor nhr-25. *Cell Metab*. 2010;12(4):398–410.
17. Musille PM, Pathak MC, Lauer JL, Hudson WH, Griffin PR, Ortlund EA. Antidiabetic phospholipid-nuclear receptor complex reveals the mechanism for phospholipid-driven gene regulation. *Nat Struct Mol Biol*. 2012;19(5):532–537.
18. Lee JM, et al. A nuclear-receptor-dependent phosphatidylcholine pathway with antidiabetic effects. *Nature*. 2011;474(7352):506–510.
19. Derks TG, et al. Inhibition of mitochondrial fatty acid oxidation in vivo only slightly suppresses gluconeogenesis but enhances clearance of glucose in mice. *Hepatology*. 2008;47(3):1032–1042.
20. Lee YK, Moore DD. Dual mechanisms for repression of the monomeric orphan receptor liver receptor homologous protein-1 by the orphan small heterodimer partner. *J Biol Chem*. 2002;277(4):2463–2467.
21. Postic C, et al. Cloning and characterization of the mouse glucokinase gene locus and identification of distal liver-specific DNase I hypersensitive sites. *Genomics*. 1995;29(3):740–750.
22. Postic C, et al. Dual roles for glucokinase in glucose homeostasis as determined by liver and pancreatic beta cell-specific gene knock-outs using Cre recombinase. *J Biol Chem*. 1999;274(1):305–315.
23. Dentin R, et al. Hepatic glucokinase is required for the synergistic action of ChREBP and SREBP-1c on glycolytic and lipogenic gene expression. *J Biol Chem*. 2004;279(19):20314–20326.
24. Dentin R, et al. Glucose 6-phosphate, rather than xylulose 5-phosphate, is required for the activation of ChREBP in response to glucose in the liver. *J Hepatol*. 2012;56(1):199–209.
25. Li MV, et al. Glucose-6-phosphate mediates activation of the carbohydrate responsive binding protein (ChREBP). *Biochem Biophys Res Commun*. 2010;395(3):395–400.
26. Fayard E, Auwerx J, Schoonjans K. LRH-1: an orphan nuclear receptor involved in development, metabolism and steroidogenesis. *Trends Cell Biol*. 2004;14(5):250–260.
27. Niswender KD, Shiota M, Postic C, Cherrington AD, Magnuson MA. Effects of increased glucokinase gene copy number on glucose homeostasis and hepatic glucose metabolism. *J Biol Chem*. 1997;272(36):22570–22575.
28. Iynedjian PB. Mammalian glucokinase and its gene. *Biochem J*. 1993;293(pt 1):1–13.
29. Kim TH, et al. Interrelationship between liver X receptor alpha, sterol regulatory element-binding protein-1c, peroxisome proliferator-activated receptor gamma, and small heterodimer partner in the transcriptional regulation of glucokinase gene expression in liver. *J Biol Chem*. 2009;284(22):15071–15083.
30. Oosterveer MH, et al. Lxralpha deficiency hampers the hepatic adaptive response to fasting in mice. *J Biol Chem*. 2008;283(37):25437–25445.
31. Denechaud PD, et al. ChREBP, but not LXRs, is required for the induction of glucose-regulated genes in mouse liver. *J Clin Invest*. 2008;118(3):956–964.
32. Liang G, Yang J, Horton JD, Hammer RE, Goldstein JL, Brown MS. Diminished hepatic response to fasting/refeeding and liver X receptor agonists in mice with selective deficiency of sterol regulatory element-binding protein-1c. *J Biol Chem*. 2002;277(11):9520–9528.
33. Park YJ, et al. Dissociation of diabetes and obesity in mice lacking orphan nuclear receptor small heterodimer partner. *J Lipid Res*. 2011;52(12):2234–2244.
34. Seoane J, Gomez-Foix AM, O'Doherty RM, Gomez-Ara C, Newgard CB, Guinovart JJ. Glucose 6-phosphate produced by glucokinase, but not hexokinase I, promotes the activation of hepatic glycogen synthase. *J Biol Chem*. 1996;271(39):23756–23760.
35. O'Doherty RM, Lehman DL, Seoane J, Gomez-Foix AM, Guinovart JJ, Newgard CB. Differential metabolic effects of adenovirus-mediated glucokinase

and hexokinase I overexpression in rat primary hepatocytes. *J Biol Chem*. 1996;271(34):20524–20530.
36. Bandsma RH, et al. Enhanced glucose cycling and suppressed de novo synthesis of glucose-6-phosphate result in a net unchanged hepatic glucose output in ob/ob mice. *Diabetologia*. 2004;47(11):2022–2031.
37. Hron WT, Sobocinski KA, Menahan LA. Enzyme activities of hepatic glucose utilization in the fed and fasting genetically obese mouse at 4-5 months of age. *Horm Metab Res*. 1984;16(suppl 1):32–36.
38. Yen TT, Stamm NB. Constitutive hepatic glucokinase activity in db/db and ob/ob mice. *Biochim Biophys Acta*. 1981;657(1):195–202.
39. Dentin R, et al. Liver-specific inhibition of ChREBP improves hepatic steatosis and insulin resistance in ob/ob mice. *Diabetes*. 2006;55(8):2159–2170.
40. Peter A, et al. Hepatic glucokinase expression is associated with lipogenesis and fatty liver in humans. *J Clin Endocrinol Metab*. 2011;96(7):E1126–E1130.
41. Scott DK, et al. A modest glucokinase overexpression in the liver promotes fed expression levels of glycolytic and lipogenic enzyme genes in the fasted state without altering SREBP-1c expression. *Mol Cell Biochem*. 2003;254(1–2):327–337.
42. Manno CS, et al. Successful transduction of liver in hemophilia by AAV-Factor IX and limitations imposed by the host immune response. *Nat Med*. 2006;12(3):342–347.
43. Ayuso E, et al. High AAV vector purity results in serotype- and tissue-independent enhancement of transduction efficiency. *Gene Ther*. 2010; 17(4):503–510.
44. Lock M, et al. Characterization of a recombinant adeno-associated virus type 2 Reference Standard Material. *Hum Gene Ther*. 2010;21(10):1273–1285.
45. Kuipers F, Havinga R, Bosschieter H, Toorop GP, Hindriks FR, Vonk RJ. Enterohepatic circulation in the rat. *Gastroenterology*. 1985;88(2):403–411.
46. Van Dijk TH, Boer TS, Havinga R, Stellaard F, Kuipers F, Reijngoud DJ. Quantification of hepatic carbohydrate metabolism in conscious mice using serial blood and urine spots. *Anal Biochem*. 2003; 322(1):1–13.
47. Lee WN, Byerley LO, Bergner EA, Edmond J. Mass isotopomer analysis: theoretical and practical considerations. *Biol Mass Spectrom*. 1991;20(8):451–458.
48. Bligh EG, Dyer WJ. A rapid method of total lipid extraction and purification. *Can J Biochem Physiol*. 1959;37(8):911–917.
49. Oosterveer MH, et al. High fat feeding induces hepatic fatty acid elongation in mice. *PLoS One*. 2009;4(6):e6066.
50. Hohorst HJ. D-Glucose-6-phosphat und D-fructose-6-phosphat. In: Bergmeyer HU, ed. *Methoden der Enzymatischen Analyse*. Weinheim, Germany; Verlag Chemie: 1970:1200–1204.
51. Keppler D, Decker K. Glykogen. Bestimmung mit amyloglucosidase. In: Bergmeyer HU, ed. *Methoden der Enzymatischen Analyse*. Weinheim, Germany; Verlag Chemie: 1970:1089–1094.
52. Mullin JM, McGinn MT, Snock KV, Kofeldt LM. Na+-independent sugar transport by cultured renal (LLC-PK1) epithelial cells. *Am J Physiol*. 1989; 257(1 pt 2):F11–F17.
53. Gauthier K, et al. Thyroid hormone receptor beta (TRbeta) and liver X receptor (LXR) regulate carbohydrate-response element-binding protein (ChREBP) expression in a tissue-selective manner. *J Biol Chem*. 2010;285(36):28156–28163.
54. Duggavathi R, et al. Liver receptor homolog 1 is essential for ovulation. *Genes Dev*. 2008;22(14):1871–1876.
55. Liang Y, Jetton TL, Zimmerman EC, Najafi H, Matschinsky FM, Magnuson MA. Effects of alternate RNA splicing on glucokinase isoform activities in the pancreatic islet, liver, and pituitary. *J Biol Chem*. 1991;266(11):6999–7007.
56. Coste A, et al. LRH-1-mediated glucocorticoid synthesis in enterocytes protects against inflammatory bowel disease. *Proc Natl Acad Sci U S A*. 2007;104(32):13098–13103.